Journal of Catalysis **184,** 157–171 (1999)
Article ID jcat.1999.2444, available online at http://www.idealibrary.com on IDEAL®

An Infrared Emission Spectroscopic Study of the Thermal Transformation Mechanims in Al_{13}-Pillared Clay Catalysts with and without Tetrahedral Substitutions

J. Theo Kloprogge,[1] Robyn Fry, and Ray L. Frost

Centre for Instrumental and Developmental Chemistry, Queensland University of Technology, 2 George Street, GPO Box 2434, Brisbane, Queensland 4001, Australia

Received October 15, 1998; revised January 21, 1999; accepted January 21, 1999

Pillaring of smectites with Al_{13} was studied *in situ* by infrared emission spectroscopy. Exchange of montmorillonite with Al_{13} gave Al–OH and Al–H_2O OH-stretching modes of Al_{13} at 3682 and 3538 cm^{-1} and at 3641 and 3334 cm^{-1} for Al_{13}-hectorite. Al_{13} conversion resulted in removal of the Al–OH mode >400°C. The Al–H_2O band was replaced by bands at 3574 and 3505 cm^{-1}, due to structural rearrangement within Al_{13}. The intensities diminished, but are still observed at 800°C, suggesting that the pillar structure incompletely converted to "Al_2O_3." In hectorite the Al_{13} completely converted upon calcination. Below 1750 cm^{-1} the Al_{13}–montmorillonite displays bands at 642, 1008, 1321, 1402, and 1512 cm^{-1}. The 1512 cm^{-1} band disappeared at 500°C, followed by the other bands above 600°C. The 642 cm^{-1} band intensity diminished but is still observed at 800°C. At 700°C a new band is observed at 722 cm^{-1} due to Al–O bond formation. The Al_{13}–hectorite displays bands at 1227, 1315, 1395, and 1510 cm^{-1}. The last three band intensities diminished but remained visible. The 1227 cm^{-1} band disappeared above 500°C. Expansion of saponite with Al_{13} gave bands at 3626 and 3244 cm^{-1}, which disappeared at 700°C, indicating that the transition to "Al_2O_3" is complete. The Mg–OH band is not influenced by calcination, indicating that the pillaring does not involve the octahedral clay layer. Below 1750 cm^{-1} Al_{13}–saponite shows bands at 1316, 1424, and 1521 cm^{-1}. Calcination resulted in a disappearance of the 1521 and 1316 cm^{-1} bands at 600°C, while the 1424 cm^{-1} band disappeared at 400°C. The 1316 cm^{-1} band is replaced by bands at 1269, 1314, and 1388 cm^{-1} above 600°C, due to formation of $M^{[IV]}$–O(H)–$Al^{[VI]}$ linkages between pillars and tetrahedral clay layers.

Key Words: **Al_{13}; hectorite; infrared emission spectroscopy; montmorillonite; pillared clay; saponite; thermal transformation.**

INTRODUCTION

Since the introduction in the 1970s metal–oxide pillared clays are prepared by the intercalation of smectites with large inorganic polymers of Al, Zr, Ti, Si, etc. (1–3). Thermal treatment of the expanded clay converts the inorganic polycations in the clay interlayer into nanoscopic metal–oxide clusters bonded to the clay. The resulting microporous material has both molecular sieving and catalytic, i.e., acidic properties. The insertion of $[AlO_4Al_{12}(OH)_{24}(H_2O)_{12}]^{7+}$ (Al_{13}) as pillaring species is well established (4). However, the mechanism how the pillars are linked to the clay during the thermal transformation of the Al_{13} to the "Al_2O_3" remains a matter of debate (4).

Significant differences exist between the models for various Al-pillared smectites. Based on ^{27}Al and ^{29}Si solid-state MAS-NMR for beidellite, a tetrahedrally substituted smectite, a mechanism was proposed in which linkages are formed between the pillar and the tetrahedral clay layer by inversion of a Si tetrahedron or a Si–O–Al bond in a tetrahedron (7). However, no reactions between pillar and tetrahedral layer were observed for smectites without tetrahedral substitutions. In contrast, Pinnavaia *et al.* (8) observed a structural transformation upon calcination of intercalated fluor–hectorite and concluded that the structural F partly replacing the OH groups in the structure causes the Si–O bands to become more labile. These labile Si–O bands then promote coupling to the Al_{13} pillar during the thermal transformation.

Spectroscopic techniques are strong tools for studying the bonding mechanisms in pillared clays on a molecular scale. Michot *et al.* (9) described the IR spectrum of the Al_{13} in solution with OH-stretching modes at 3438 and 3180 cm^{-1}, OH-bending modes at 1640 (H_2O), 1085, and 979 cm^{-1}, and other OH-modes at 772, 695, 582, and 530 cm^{-1}. The IR spectrum of Al_{13}-sulfate showed an Al–OH stretching band at 3440 cm^{-1}, H–OH stretching band at 3247 cm^{-1}, H–OH deformation mode at 1640 cm^{-1}, Al–OH bending and deformation modes at 1085 and 980 cm^{-1}, and the AlO_4 asymmetric and symmetric stretching modes at 780 and 636 cm^{-1} (10–12). Brydon and Kodama (13) described the formation of new OH-stretching bands at 3700 and 3480 cm^{-1} for Al-pillared montmorillonite, which disappeared after heating to 450 and 590°C.

[1] To whom correspondence should be addressed. Fax: +61 7 3864 1804. E-mail: t.kloprogge@qut.edu.au.

0021-9517/99 $30.00

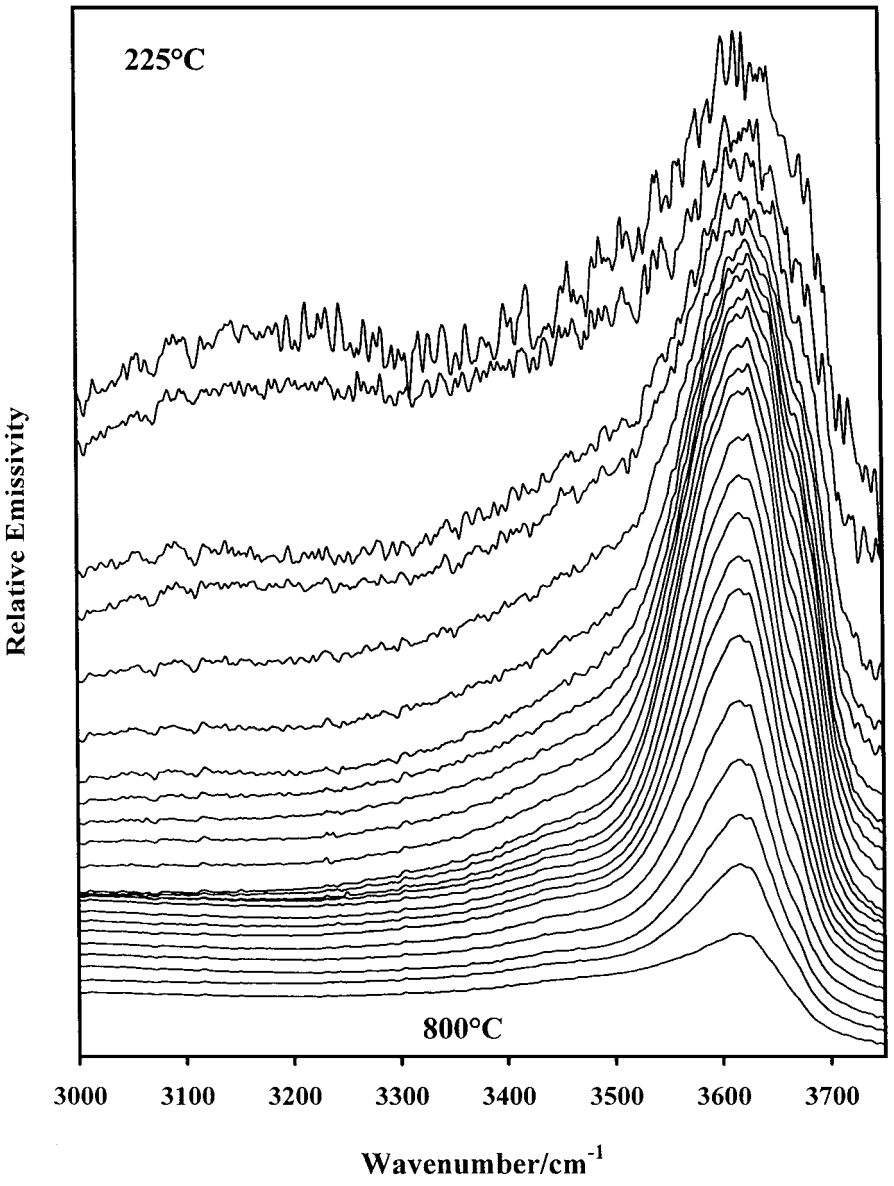

FIG. 1. IES spectra in the hydroxyl-stretching region of Al_{13}-pillared montmorillonite in the range 225–800°C at 25°C intervals.

Similar bands were observed by Goh and Huang (14) at 3695 and 3570 cm^{-1}. In contrast, Gupta and Malik (15) observed totally different bands at 2750, 2445, and 908 and a shoulder at 1315 cm^{-1}. They concluded that this pointed toward the development of new atomic grouping and possible transformation of the original clay structure. Tennakoon *et al.* (16) did not observe any new bands but found a progressive decrease in intensity of the structural OH– stretching mode at 3630 cm^{-1} and Al–OH–Al and Al–O–Mg librational modes at 913 and 844 cm^{-1}. At 500°C a drastic reduction in intensity of the 3630 cm^{-1} band was thought to be unique for pillared clays. They postulated a model in which condensation of the terminal OH groups of the Al_{13} complex with the lattice OH groups on the clay sheets. The oxide pillars then become directly linked via oxygens to the Al and Mg atoms in the octahedral layer of the montmorillonite. Tichit *et al.* (17) observed that exchange with Al_{13} had no effect on the tetrahedral layer of the montmorillonite based especially on the absence of changes in the 1125 cm^{-1} ($Si–O^{apical}$ stretching mode), the 1035 cm^{-1} (combined stretching and bending modes $Si–O^{basal}$), and the 935 cm^{-1} (Al–OH) bands. A slight shift of the 710 cm^{-1} band toward 735 cm^{-1} was the only change in the infrared spectrum. Kloprogge *et al.* (18) found only a slight increase in intensity of the Al–OH and (Mg, Al)–OH modes at 921 and 849 cm^{-1}, respectively, for pillared montmorillonite. Calcination at 400°C resulted in a decrease in intensity of all bands associated

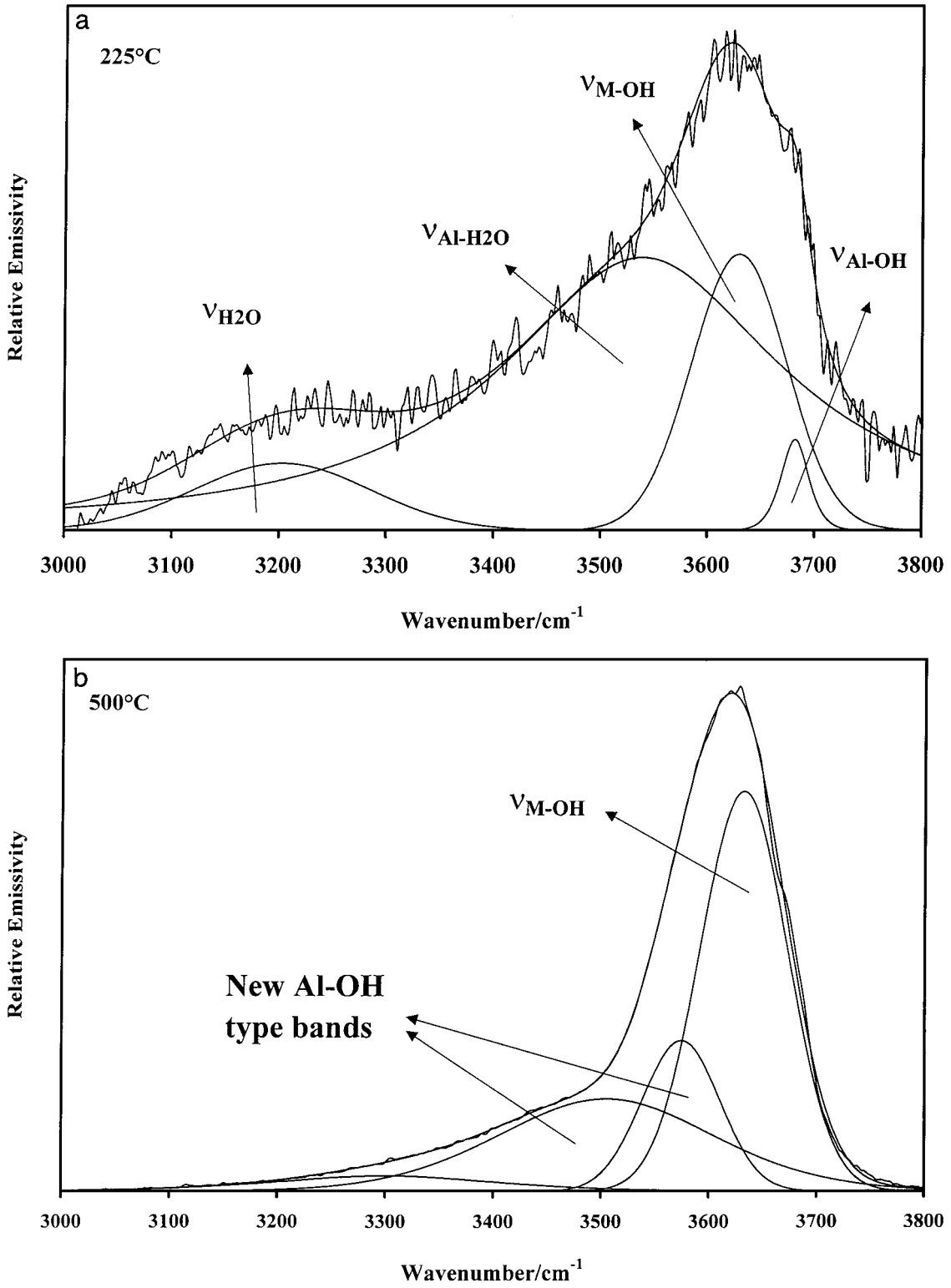

FIG. 2. Band component analysis of the infrared emission hydroxyl stretching region of (a) Al_{13}-exchanged montmorillonite at 225°C and (b) Al_{13}-pillared montmorillonite at 500°C.

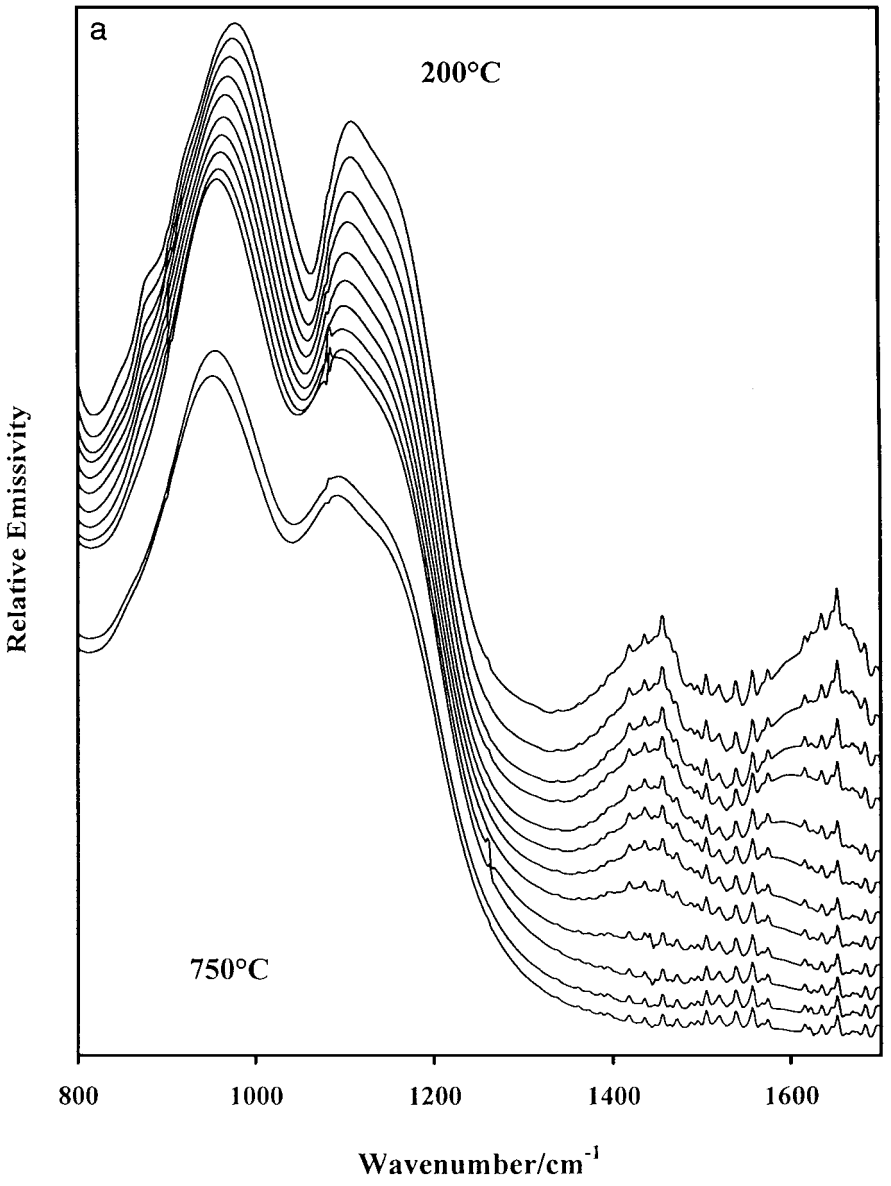

FIG. 3. IES spectra in the 800 to 1700 cm^{-1} region of (a) montmorillonite Swy-1 in the range 200–750°C at 50°C intervals and (b) its Al_{13}-pillared analog in the range 200–800°C at 25°C intervals.

with hydroxyl groups and the formation of a new band around 3456 cm^{-1} in the hydroxyl-stretching region, which was not observed during calcination of normal montmorillonite. For pillared beidellite Kloprogge *et al.* (18) observed reductions in intensities of the 3651 cm^{-1} Al–OH stretching mode and the 937 cm^{-1} Al–OH libration mode. At 200°C a new band at 3453 cm^{-1} seemed to develop analogs to the pillared montmorillonite but with a much stronger intensity. This band was also observed by Schutz *et al.* (19) as a shoulder after heating to 100°C on a broad band around 3640 cm^{-1}, which they believe to contain at least three different contributions at 3640, 3620, and 3600 cm^{-1}. They assigned this band to Si–OH groups created by the breaking of Si–O–$Al^{[IV]}$ bonds. Adsorption of pyridine resulted in the disappearance of this band, indicating that the corresponding site was available to pyridine to adsorb. Li *et al.* (20) reported the infrared spectra of Al_{13}-pillared synthetic saponites. Exchange of the saponite with Al_{13} resulted in a shift toward higher frequencies for the 1054 and 988 cm^{-1} bands assigned to the Si(Al)–O stretching modes and toward lower frequencies for the 738 and 652 cm^{-1} bands assigned to Si–O–Al modes. Further, a reduction in intensity of the 820 and 691 cm^{-1} bands was observed. Calcination of the exchanged saponite resulted mainly in a decrease in intensity of the Si–O–Al bending mode at 646 cm^{-1}. This decrease was interpreted to be caused by a reaction between

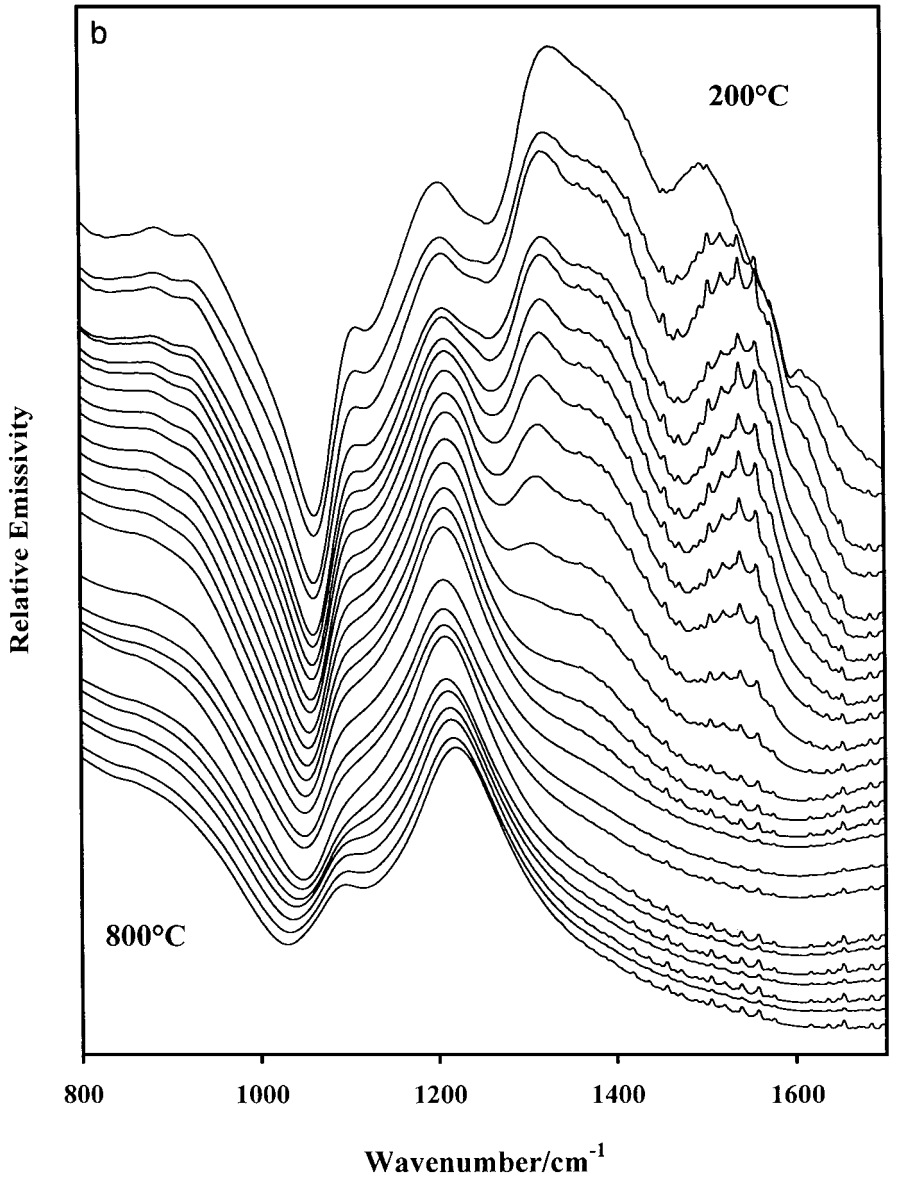

FIG. 3—*Continued*

the Al_{13} pillar and the tetrahedral clay layers probably on Si–O–Al linkages. Chevalier *et al.* (21) reported a new band in the OH-stretching region around 3594 to 3597 cm^{-1}, which they interpreted as a new OH– type created by the pillaring process comparable to the band observed by Ocelli and Finseth (22) for H-bonded OH-groups in pillared hectorite.

Infrared emission spectroscopy (IES) has not been used before to study the structural changes *in situ* during the calcination of the Al_{13}-expanded clay, although the technique is known for the study of other solid materials like minerals. Until now expanded clays were calcined at specific temperatures, quenched, and then used for IR studies. IES is based on measuring discrete vibrational frequencies emitted by thermally excited molecules and has the major advantage that the spectra are measured *in situ* at elevated temperatures without sample preparation, calcination, and quenching procedures prior to the measurements. In this paper we describe the results of *in situ* infrared emission measurements during the thermal transformation of three different Al_{13}-exchanged clays with tetrahedral substitutions (saponite) and without tetrahedral substitutions (montmorillonite and hectorite). The objective of this paper is first to show the transformation of the Al_{13} complex to the metal–oxide pillar and second to show the differences in linkage mechanisms between tetrahedrally substituted and octahedrally substituted clays. In the end, detailed knowledge of the transformation mechanisms and the linkage types occurring in pillared clays will enable future workers to design tailor-made catalysts based on pillared clays.

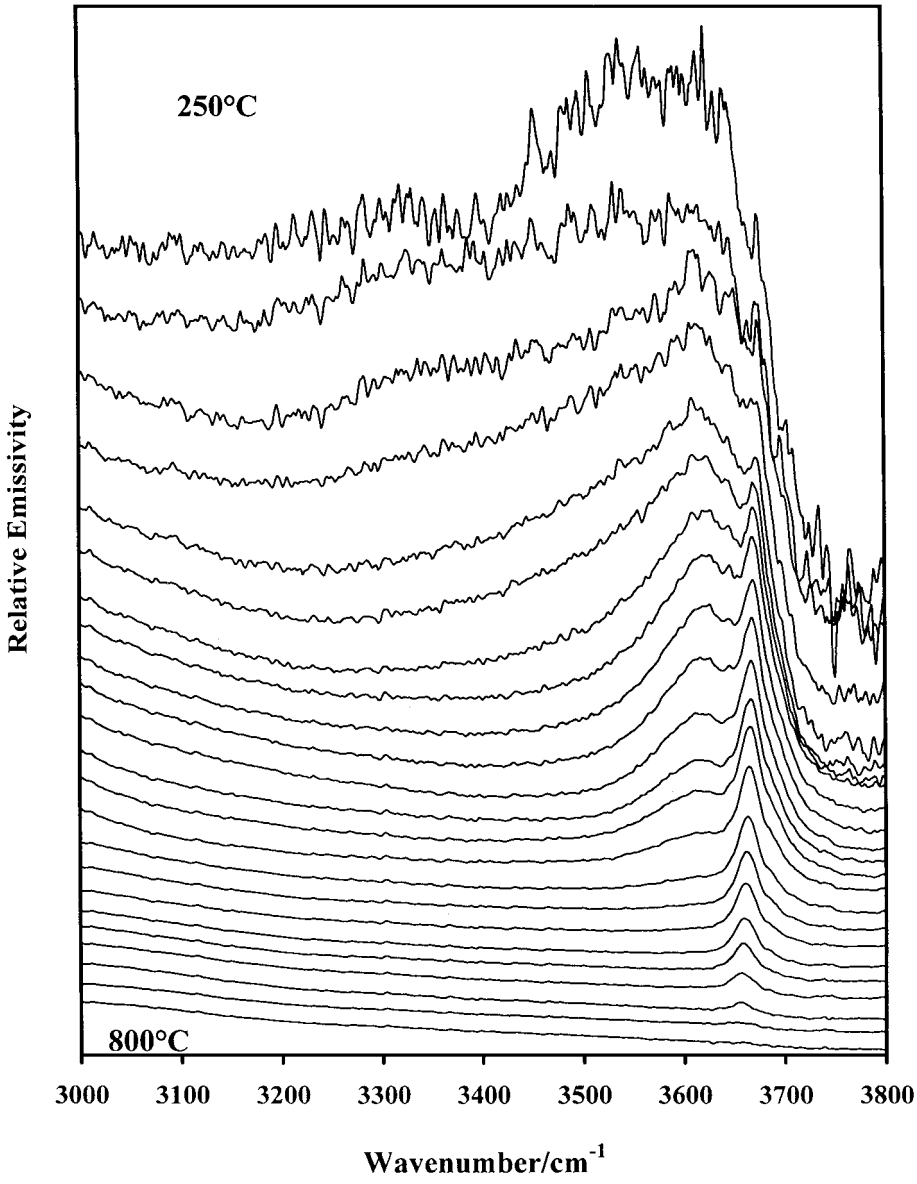

FIG. 4. IES spectra in the hydroxyl-stretching region of Al_{13}-pillared hectorite in the range 250–800°C at 25°C intervals.

METHODS

In this study Al_{13} solutions were prepared by forced hydrolysis of an $Al(NO_3)_3$ solution by slowly injecting a NaOH solution until an OH/Al molar ratio of 2.4 was reached (18, 23). As starting clays Na-saturated montmorillonite Swy-1 (Wyoming bentonite) and hectorite SHCa-1 from the Clay Minerals Society Source Clay Repository and saponite from Milford (Utah) were used. The Al_{13}-exchanged clays were prepared by mixing 20 g/L Na-saturated clay suspensions with the Al_{13} solution. The Al_{13}-exchanged clays were washed five times to remove excess ions and to improve the pillaring of the clay (24). Finally, the clays were air-dried before X-ray diffraction and IES. The XRD showed increased basal spacings from around 12.5 to around 18.5 Å for the expanded montmorillonite, saponite, and hectorite.

FTIR emission spectroscopy was carried out on a Digilab FTS-60A spectrometer, which was modified by replacing the IR source with an emission cell. A description of the cell and principles of the emission experiment have been published elsewhere (25–27). Approximately 0.2 mg of the Al_{13}-expanded clay sample was spread as a thin layer on a 6-mm-diameter platinum surface and held in an inert atmosphere within a nitrogen-purged cell during heating. The infrared emission cell consists of a modified atomic absorption graphite rod furnace, which is driven by a thyristor-controlled AC power supply capable of delivering up to

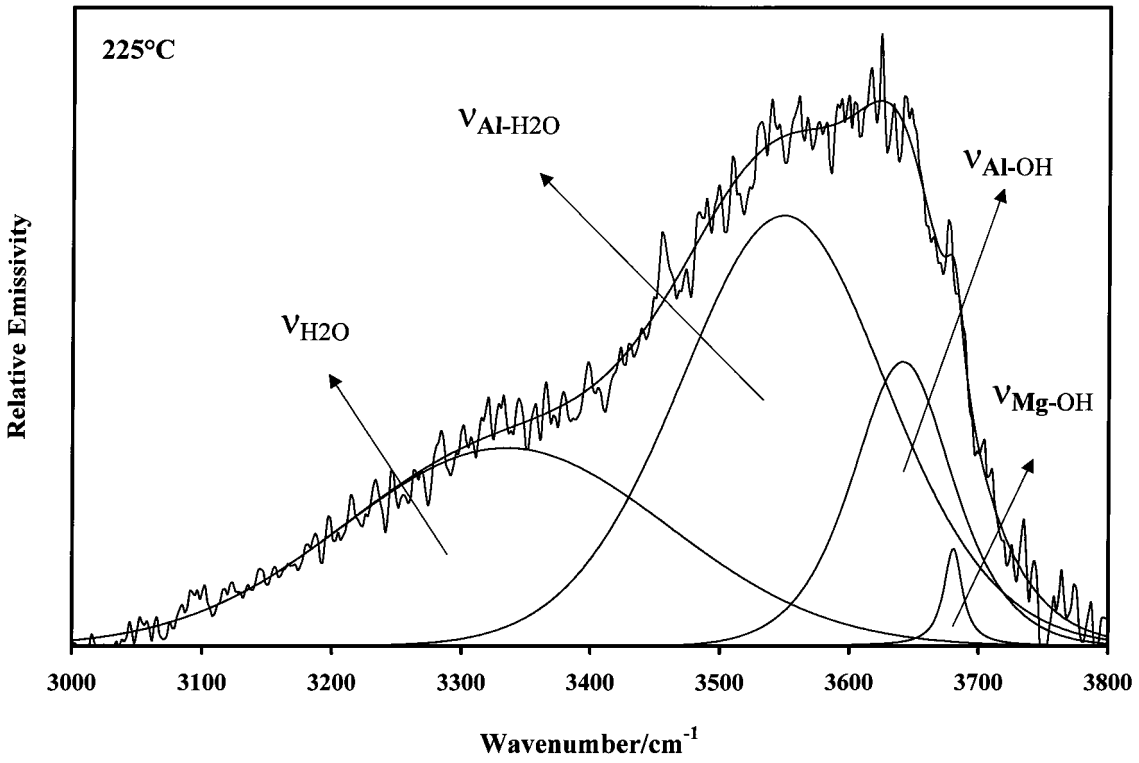

FIG. 5. Band component analysis of the infrared emission hydroxyl stretching region of Al_{13}-exchanged hectorite at 225°C.

150 amps at 12 volts. A platinum disk acts as a hot plate to heat the sample and is placed on the graphite rod. An insulated 125-μm type R thermocouple was embedded inside the platinum plate in such a way that the thermocouple junction was <0.2 mm below the surface of the platinum. Temperature control of ±2°C at the operating temperature of the sample was achieved by using an Eurotherm Model 808 proportional temperature controller, coupled to the thermocouple.

The design of the IES facility is based on an off axis paraboloidal mirror with a focal length of 25 mm mounted above the heater captures the infrared radiation and directs the radiation into the spectrometer. The assembly of the heating block and platinum hot plate is located such that the surface of the platinum is slightly above the focal point of the off axis paraboloidal mirror. By this means the geometry is such that an approximately 3-mm-diameter area is sampled by the spectrometer. The spectrometer was modified by the removal of the source assembly and mounting of a gold-coated mirror, which was drilled through the center to allow the passage of the laser beam. The mirror was mounted at 45°, which enables the IR radiation to be directed into the FTIR spectrometer.

In the normal course of events, three sets of spectra are obtained: first, the blackbody radiation over the temperature range selected at the various temperatures, second, the platinum plate radiation is obtained at the same temperatures, and third, the spectra from the platinum plate covered with the sample. Normally only one set of blackbody and platinum radiation is required. The emittance spectrum at a particular temperature was calculated by subtraction of the single beam spectrum of the platinum backplate from that of the platinum + sample, and the result ratioed to the single beam spectrum of an approximate blackbody (graphite). This spectral manipulation is carried out after all the spectral data has been collected.

The emission spectra were collected at intervals of either 25°C (pillared samples) or 50°C (standard clay samples) over the range 200–750°C. The time between scans (while the temperature was raised to the next hold point) was approximately 100 s. It was considered that this was sufficient time for the heating block and the powdered sample to reach temperature equilibrium. The spectra were acquired by coaddition of 64 scans for the whole temperature range (approximate scanning time 45 s), with a nominal resolution of 4 cm^{-1}. Good quality spectra can be obtained providing that the sample thickness is not too large. If too large a sample is used then the spectra become difficult to interpret as a result of reabsorption. Spectral manipulation such as baseline adjustment, smoothing, and normalization was performed using the Spectracalc software package GRAMS (Galactic Industries Corporation, NH). IES band positions and intensities of the bands have been determined by band component analysis using the Jandel "Peakfit" software package.

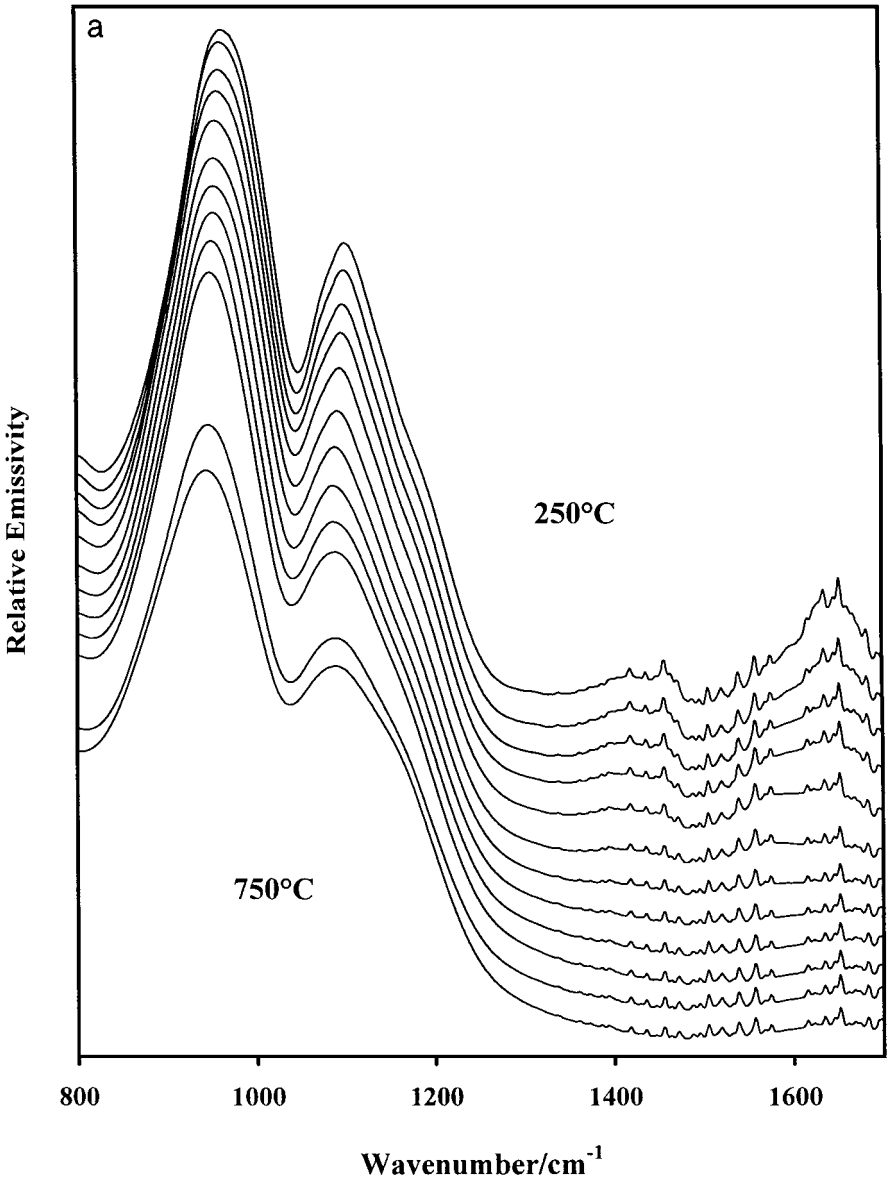

FIG. 6. IES spectra in the 800 to 1700 cm^{-1} region of (a) hectorite in the range 200–750°C at 50°C intervals and (b) its Al_{13}-pillared analog in the range 200–800°C at 25°C intervals.

RESULTS AND DISCUSSION

Pillared Montmorillonite

Figure 1 shows the hydroxyl-stretching region of the infrared emission spectra of the Al_{13}-expanded montmorillonite. In the hydroxyl-stretching region the Swy-1 montmorillonite is characterized by two bands at 3628 and 3363 cm^{-1} assigned to the M–OH and interlayer H_2O OH-stretching modes. Exchange with the Al_{13} complex resulted in two new bands at 3682 and 3538 cm^{-1}, which represent the Al–OH and Al–H_2O OH-stretching modes of the Al_{13}–complex (Fig. 2a). The Al–OH band was previously observed around 3695 and 3700 cm^{-1} in infrared absorption spectra (13, 15). The Al–H_2O band belonging to the Al_{13} was observed before at 3570 cm^{-1} by Goh and Huang (15). The interlayer water band strongly diminished in intensity after the exchange with Al_{13}. Calcination resulted in the rapid disappearance of the remaining interlayer water. The transformation of the Al_{13} complex resulted in the disappearance of the Al–OH stretching band between 400 and 500°C. In the same temperature interval the Al–H_2O OH-stretching band was replaced by two new bands around 3574 and 3505 cm^{-1}, indicating a structural rearrangement within the Al_{13} complex (Fig. 2b). Although these bands strongly diminished in intensity they are still observed at

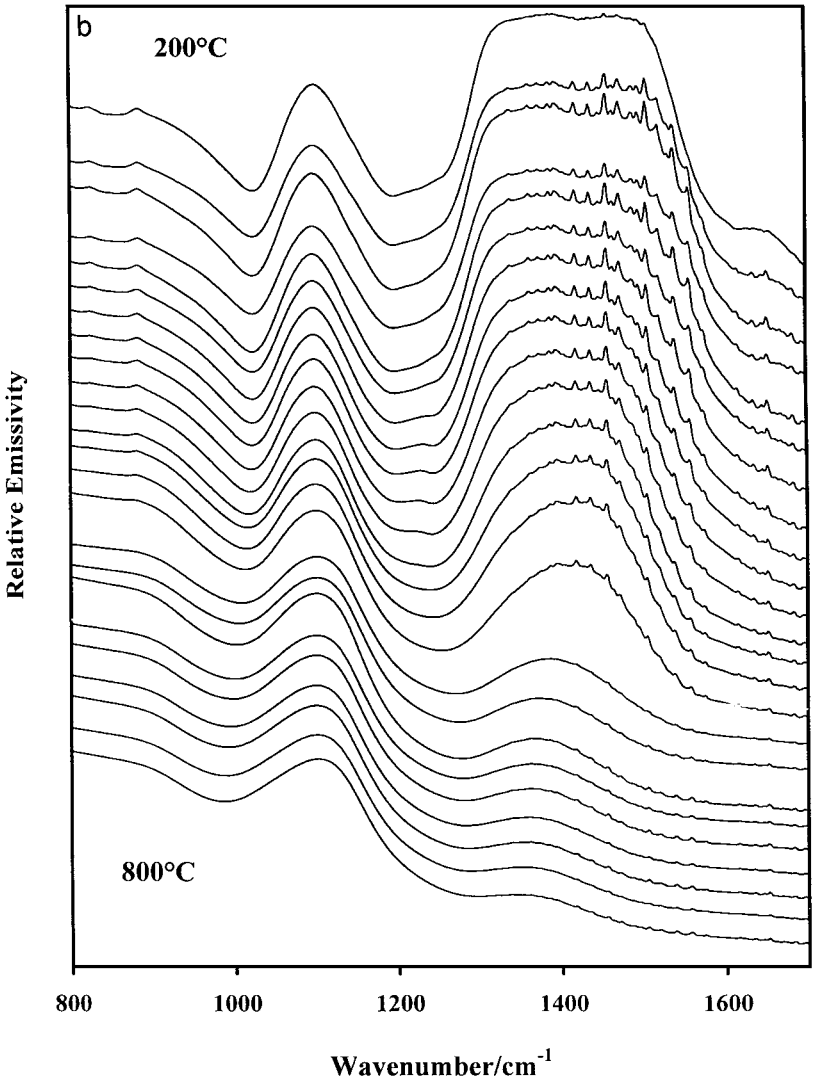

FIG. 6—*Continued*

800°C, which suggests that the pillar structure still contains some structural OH-groups and has not completely converted to aluminum oxide as generally assumed. These bands may represent OH bridges between adjacent partly dehydroxylated Al_{13} molecules. The M–OH band remained visible in the entire temperature range without changes in position but with decreasing intensity when the dehydroxylation of the clay proceeds. The clay showed complete dehydroxylation above 700°C. The thermal stability is slightly increased upon pillaring as evidenced by the incomplete dehydroxylation at 800°C.

The changes in the low frequency region during the thermal treatment of both the montmorillonite and its Al_{13}-exchanged analog are shown in Fig. 3. In the low frequency region the Al_{13}-exchanged montmorillonite displays new bands at 642, 1008, 1321, 1402 and 1512 cm^{-1} in comparison to the original montmorillonite. The first two bands correspond well with the bands observed for Al_{13}-sulfate (10). The other bands probably represent a differentiation of the initial water band of the Al_{13} complex around 1640 cm^{-1} due to the geometrical constraints of the clay interlayer causing different interactions between the various water molecules on the outside of the Al_{13} complex and the clay sheets. Molecular simulation studies have revealed that the ideal Al_{13} molecule will be oriented in the interlayer with its threefold axis perpendicular and the aluminum and oxygen plains parallel to the clay layers (28). This results in water molecules oriented toward either the clay layer above or below and toward the interlayer. The band at 1512 cm^{-1} disappeared around 500°C, followed by the bands at 1402, 1321, and 1008 cm^{-1} above 600°C. The band at 642 cm^{-1} diminished in intensity but is still observed at 800°C. At 700°C a new band is observed at 722 cm^{-1}, indicating the formation of an Al–O bond like the very strong band observed for corundum (29). The model of Tennakoon *et al.* (16), in which condensation of the terminal OH groups of

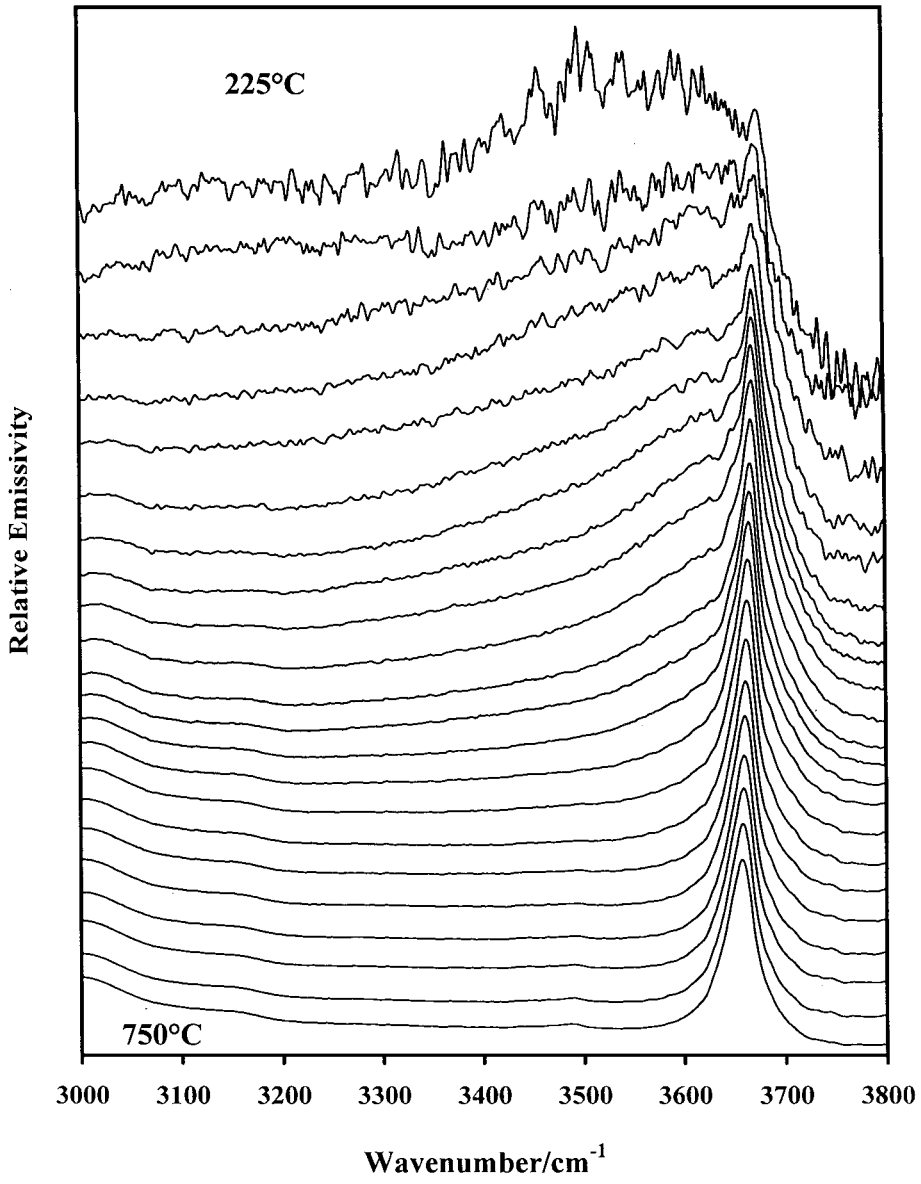

FIG. 7. Infrared emission spectra in the hydroxyl-stretching region of Al_{13}-pillared saponite in the range 225–750°C at 25°C intervals.

the Al_{13} complex with the lattice OH groups in the clay octahedral layers results in a direct linkage via oxygen to the cations (Mg or Al) in the octahedral layer, must be considered incorrect based on the above observations and the fact that this will require the formation of a very long metal(clay)–oxygen–metal(pillar) bond through the hexagonal holes in the tetrahedral layer. This seems to be very unlikely based on both the geometrical constraints and the energies involved in the formation of such a bond.

Pillared Hectorite

Figure 4 shows the hydroxyl stretching region of the infrared emission spectra of the Al_{13}-expanded hectorite. In the hydroxyl-stretching region the hectorite is characterized by two bands at 3671 and 3453 cm^{-1} assigned to the M–OH and interlayer H_2O OH-stretching modes. Exchange with the Al_{13} complex resulted in two new bands at 3641 and 3334 cm^{-1}, which must represent the Al–H_2O and Al–OH OH-stretching modes of the Al_{13} complex (Fig. 5) while the initial hectorite bands shift to 3680 and 3548 cm^{-1}. This behavior is completely comparable to that observed upon the expansion of montmorillonite as discussed above. The interlayer water band strongly diminished in intensity after the exchange with Al_{13}, which is also reflected in the 1643 cm^{-1} band. Calcination resulted in the rapid disappearance of the remaining interlayer water. The transformation of the Al_{13} complex resulted in the disappearance

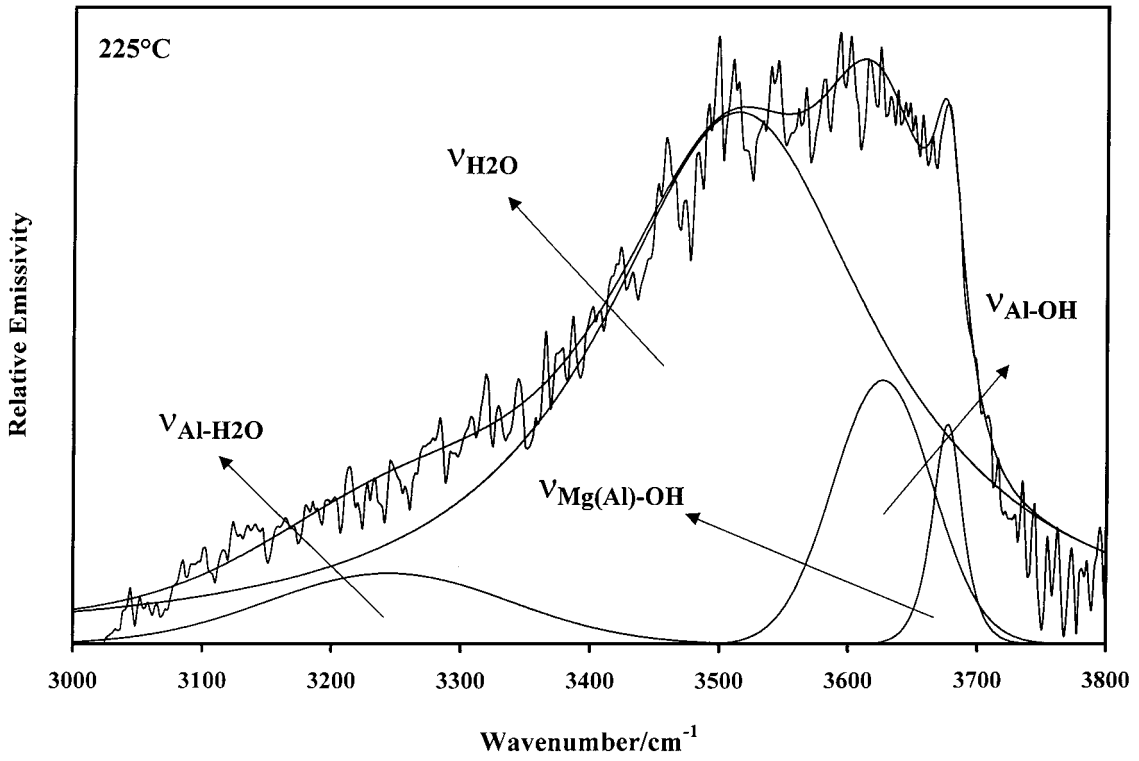

FIG. 8. Band component analysis of the infrared emission hydroxyl stretching region of Al_{13}-exchanged saponite at 225°C.

of the Al–H_2O stretching band between 400 and 500°C. In contrast to the pillared montmorillonite, the Al–OH band strongly diminished in intensity and disappeared at 600°C, which suggests that the pillar structure completely converted to aluminum oxide. The M–OH band remained visible in the entire temperature range without significant changes in position but with decreasing intensity when the dehydroxylation of the clay proceeds. The clay showed no complete dehydroxylation up to 750°C. In contrast to the pillared montmorillonite, the thermal stability seems slightly decreased upon pillaring as evidenced by the complete dehydroxylation at 750°C. This lower thermal stability is probably due to the diffusion of protons released from the pillars during dehydroxylation according to (18),

$$Al_{13} \rightarrow 6.5\,Al_2O_3 + 7H^+ + 20.5\,H_2O.$$

Moreover, the dehydroxylation of the pillars produces water, causing the local partial water pressure in the clay structure to be sufficiently high to induce hydrolysis. This effect was not observed for the pillared montmorillonite because the dehydroxylation was not completed in the temperature range studied with IES.

The changes in the low frequency region during the calcination of the hectorite and its Al_{13}-exchanged analog are shown in Fig. 6. In the low frequency region the Al_{13}-exchanged hectorite displays new bands at 1227, 1315, 1395, and 1510 cm^{-1} in comparison to the original clay. The last three bands correspond well with the bands observed for Al_{13}–montmorillonite. The small band at 1227 cm^{-1} has not been observed before in Al_{13}-exchanged clays and cannot be identified yet. Here again it is assumed that the bands comparable to the ones observed in the exchanged montmorillonite represent a differentiation of the initial water band of the Al_{13} complex around 1640 cm^{-1} due to the geometrical constraints of the clay interlayer, causing different interactions between the various water molecules on the outside of the Al_{13} complex and the clay sheets. The initial water band observed for the hectorite is strongly diminished in the Al_{13}-exchanged hectorite. The band at 1510 cm^{-1} strongly diminished in intensity but remained visible up to 800°C. A similar behavior was observed for the other two bands at 1315 and 1395 cm^{-1}. The band at 1227 cm^{-1}, however, disappeared after heating to 500°C. At high temperatures no new band was observed, like the band at 722 cm^{-1} in the pillared montmorillonite, indicating the formation of an Al–O bond. No changes in the low frequency region indicate the formation of some sort of linkage between the aluminum-oxide pillar and the clay structure. The only changes observed are due to the dehydroxylation of the clay at higher temperatures. This may indicate that the pillar is present in the form of some sort of amorphous alumina from which no vibrations are observed due to a high amount of disorder. The expanded basal spacing in

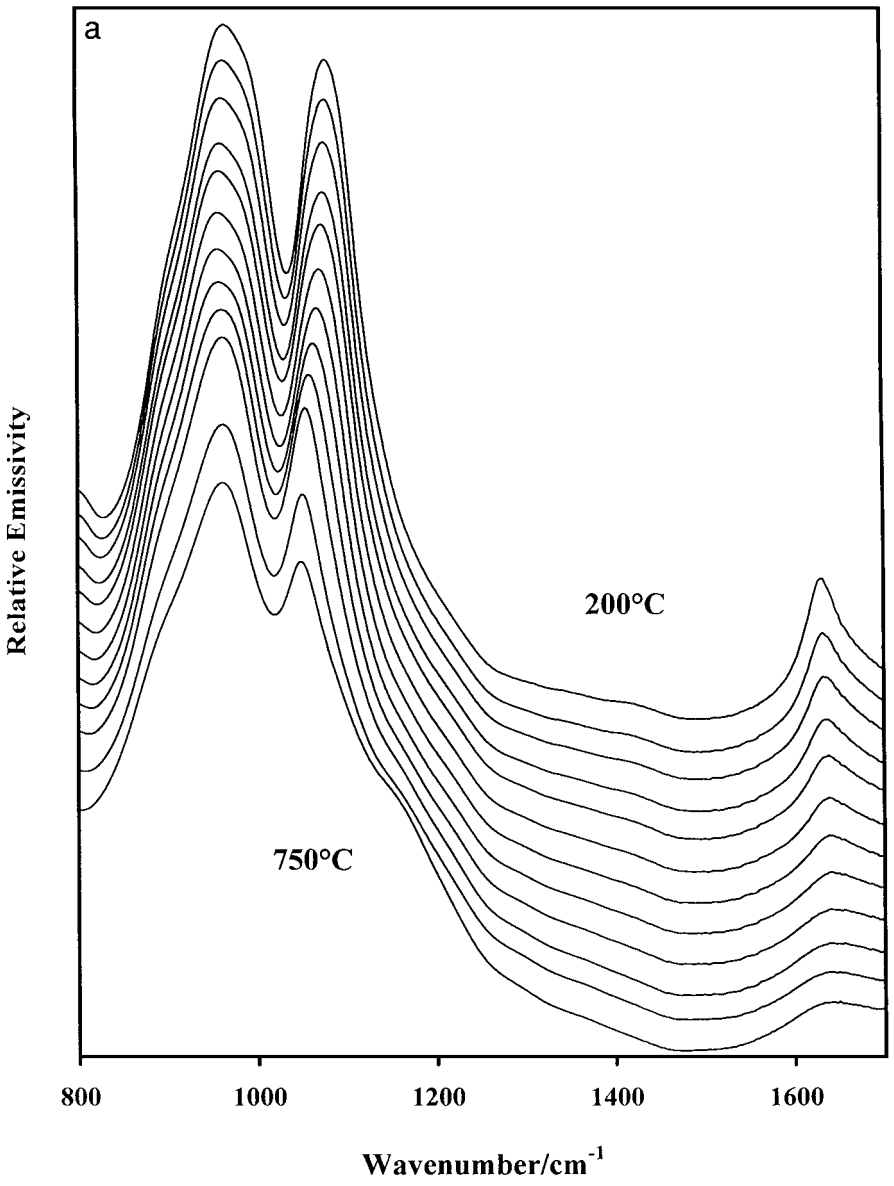

FIG. 9. IES spectra in the 800 to 1700 cm^{-1} region of (a) saponite in the range 200–750°C at 50°C intervals and (b) its Al_{13}-pillared analog in the range 200–750°C at 25°C intervals.

the XRD pattern of the thermally treated clay supports the presence of amorphous alumina as a pillar and not Al^{3+} as an interlayer cation after complete breakdown of the pillar.

Pillared Saponite

Figure 7 shows the infrared emission spectra of the Al_{13}-exchanged saponite in the hydroxyl-stretching region. Saponite displays in the hydroxyl-stretching region a sharp band at 3669 cm^{-1} and a broad band around 3490 cm^{-1} assigned to the Mg–OH (20) and the interlayer H_2O OH-stretching modes, respectively. Exchange with Al_{13} resulted in new bands at 3626 and 3244 cm^{-1} assigned to Al–H_2O and Al–OH OH-stretching modes, respectively (Fig. 8). The 3626 cm^{-1} band is comparable to the band observed for H-bonded hydroxy-groups in pillared hectorite (26). In contrast to the Al_{13}-exchanged montmorillonite both the Al–OH and the Al–H_2O bands are observed at much lower frequencies. This is probably caused by the different interlayer environment in which in saponite the layer charge is very localized in the tetrahedral layer adjacent to the pillaring molecules instead of the more diffuse layer charge on the octahedral layer in montmorillonite shielded from the pillaring molecules. Heating resulted in a strongly diminishing intensity of the interlayer water band. The Al–OH band broadened and shifted to higher frequencies and strongly

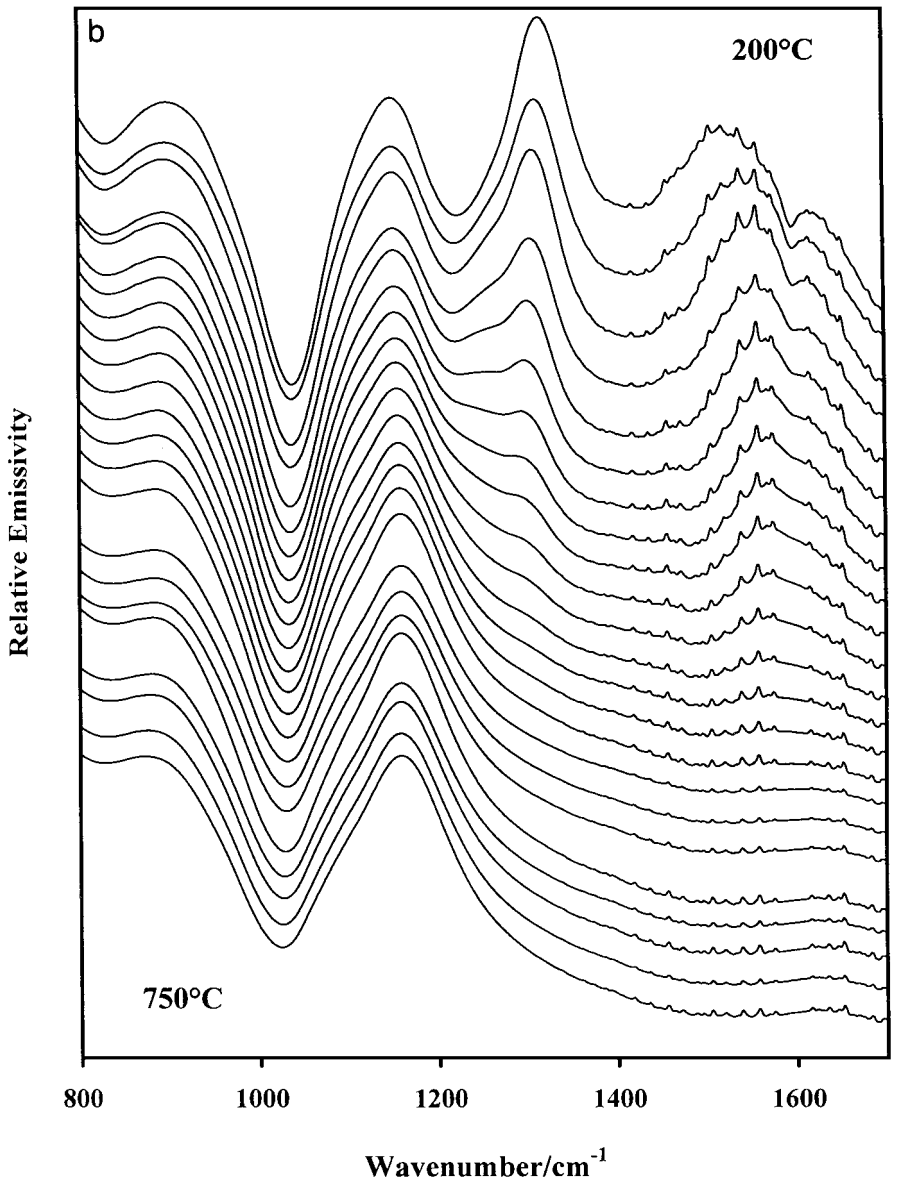

FIG. 9—*Continued*

diminished in intensity above 500°C. At 700°C this band and the Al–H_2O band have completely disappeared, indicating that in saponite the transition to aluminum oxide is complete. The Mg–OH band is hardly influenced by the calcination, indicating higher thermal stability of the pillared saponite compared to the pillared montmorillonite and the pillaring mechanism in saponites does not involve the octahedral clay layer.

The effect of the thermal treatment on the saponite and its Al_{13}-exchanged analog in the infrared emission low frequency region is shown in Fig. 9. Al_{13}-exchanged saponite shows in the low frequency region new bands at 1316, 1424, and 1521 cm^{-1} comparable with the three highest frequency bands observed for Al_{13}-exchanged montmorillonite. In contrast to the exchanged montmorillonite, calcination of the Al_{13}-exchanged saponite resulted in a disappearance of the 1521 and 1316 cm^{-1} bands around 600°C, while the 1424 cm^{-1} band disappeared around 400°C. Saponite has, just like beidellite, mainly tetrahedral substitutions and therefore the pillaring mechanism is comparable. It is assumed that during the calcination the Al_{13} complex will lose protons, which will react with the Si–O–Al in the tetrahedral layers to give Si–OH–Al and subsequent weakening of this linkage (21). Inversion of the tetrahedra or of a Si–OH–Al within a tetrahedron provides then the possibility to form pillar-layer linkages. Indications for such a linkage must be reflected in the newly formed $M^{[IV]}$–OH–$Al^{[VI]}$ or $M^{[IV]}$–O–$Al^{[VI]}$ modes in the IES low frequency

region. The initially observed band at 1316 cm^{-1} seems to be replaced above 600°C by a complex of three new weak bands around 1269, 1314, and 1388 cm^{-1}. These bands indicate the formation of such $M^{[IV]}$–O(H)–$Al^{[VI]}$ linkages between the pillars and the saponite tetrahedral layers. In general the formation and breaking up of a Si–OH–Al linkage will result in the preferential formation of an Al–OH... reactive bond, which in turn can react with the pillaring species. The observed bands can then tentatively be assigned to three different Al–O bonds with varying bond length formed upon the linkage with three Al–OH... of the clay tetrahedral layers.

CONCLUSIONS

The results presented in this paper clearly show the strength of infrared emission spectroscopy for studying *in situ* the transformations taking placing during the preparation and thermal treatment of pillared clays. Exchange of montmorillonite and hectorite with Al_{13} resulted in new Al–OH and Al–H_2O OH-stretching modes of the Al_{13} complex at 3682 and 3538 cm^{-1} and 3641 and 3334 cm^{-1}, respectively. The transformation of Al_{13} upon calcination resulted in the disappearance of the Al–OH stretching mode. The Al–H_2O OH-stretching mode was replaced by new bands around 3574 and 3505 cm^{-1}, indicating a structural rearrangement within the Al_{13} complex. In the low frequency region the Al_{13}-exchanged montmorillonite displays new bands at 642, 1008, 1321, 1402, and 1512 cm^{-1}. The bands at 1512, 1402, 1321, and 1008 cm^{-1} disappeared upon calcination above 500°C. The band at 642 cm^{-1} diminished in intensity but is still observed at 800°C. At 700°C a new band is observed at 722 cm^{-1}, indicating the formation of an Al–O bond within the pillar. No changes in the low frequency region indicate the formation of some sort of linkage between the aluminum-oxide pillar and the clay structure. Based on the IES data the model in which the complex is linked to the octahedral layer is considered to be incorrect. In hectorite the Al_{13} is completely converted to aluminum-oxide upon calcination to 800°C. The Al_{13}-exchanged hectorite is comparable to the exchanged montmorillonite and displays new bands at 1227, 1315, 1395, and 1510 cm^{-1}. At high temperatures no new band was observed, like the band at 722 cm^{-1} in the pillared montmorillonite. As for the pillared montmorillonite no changes in the low frequency region indicate the formation of some sort of linkage between the aluminum-oxide pillar and the mainly octahedrally charged clay structure. The thermal stability is slightly decreased upon pillaring due to a protonic attack on the clay structure of protons released from the pillars upon thermal treatment. Expansion of saponite with Al_{13} resulted in new bands at 3626 and 3244 cm^{-1}. At 700°C the transition of the pillar to aluminum-oxide in the saponite is complete. The Mg–OH band is hardly influenced by calcination, indicating that the pillaring mechanism in saponites does not involve the octahedral clay layer. Al_{13}-exchanged saponite shows in the low frequency region new bands at 1316, 1424, and 1521 cm^{-1}. Calcination of the Al_{13}-exchanged saponite resulted in a disappearance of the 1521, 1424, and 1316 cm^{-1} bands. The band at 1316 cm^{-1} is replaced by three new bands around 1269, 1314, and 1388 cm^{-1} above 600°C, indicating the formation of $M^{[IV]}$–O(H)–$Al^{[VI]}$ linkages between the pillars and the saponite tetrahedral layers. The bands are assigned to Al–O bonds with varying bond length formed upon the linkage with different Al–OH... groups of the tetrahedral layers.

ACKNOWLEDGMENTS

The authors thank Greg Cash for his technical assistance with the Infrared Emission Spectrometer. Prof. Graeme George is thanked for the use of the Infrared Emission Spectrometer. The financial and infrastructural support of the Queensland University of Technology, Centre for Instrumental and Developmental Chemistry, is gratefully acknowledged.

REFERENCES

1. Brindley, G. W., and Sempels, R. E., *Clay Miner.* **12**, 229 (1977).
2. Lahav, N., Shani, U., and Shabtai, J., *Clays Clay Miner.* **26**, 107 (1978).
3. Vaughan, D. E. W., U.S. Patent 4,666,877 (1987).
4. Kloprogge, J. T., *J. Porous Mater.* **5**, 5 (1998).
5. Pinnavaia, T. J., Tzou, M.-S., and Landau, S. D., *J. Am. Chem. Soc.* **107**, 4783 (1985).
6. Ohtsuka, K., *Chem. Mater.* **9**, 2039 (1997).
7. Plee, D., Borg, F., Gatineau, L., and Fripiat, J. J., *J. Am. Chem. Soc.* **107**, 2362 (1985).
8. Pinnavaia, T. J., Landau, S. D., Tzou, M.-S., and Johnson, I. D., *J. Am. Chem. Soc.* **107**, 7222 (1985).
9. Michot, L. J., Barrès, O., Hegg, E. L., and Pinnavaia, T. J., *Langmuir* **9**, 1794 (1993).
10. Kloprogge, J. T., Geus, J. W., Jansen, J. B. H., and Seykens, D., *Thermochimica Acta* **209**, 265 (1992).
11. Kloprogge, J. T., and Frost, R. L., *Thermochim. Acta* **320**, 245 (1998).
12. Teagarden, T. L., Kozlowski, J. F., and White, J. L., *J. Pharm. Sci.* **70**, 758 (1981).
13. Brydon, J. E., and Kodama, H., *Am. Miner.* **51**, 875 (1966).
14. Goh, T. B., and Huang, P. M., *Clays Clay Miner.* **34**, 37 (1986).
15. Gupta, G. C., and Malik, W. U., *Am. Miner.* **54**, 1625 (1969).
16. Tennakoon, D. T. B., Jones, W., and Thomas, J. M., *J. Chem. Soc. Faraday Trans.* **82**, 3081 (1986).
17. Tichit, D., Fajula, F., Figueras, F., Ducourant, B., Mascherpa, G., Gueguen, C., and Bousquet, J., *Clays Clay Miner.* **36**, 369 (1988).
18. Kloprogge, J. T., Booij, E., Jansen, J. B. H., and Geus, J. W., *Clay Miner.* **29**, 153 (1994).
19. Schutz, A., Stone, W. E. E., Poncelet, G., and Fripiat, J. J., *Clays Clay Miner.* **35**, 251 (1987).
20. Li, L., Liu, X., Ge, Y., Xu, R., Rocha, J., and Klinowski, J., *J. Phys. Chem.* **97**, 10389 (1993).
21. Chevalier, S., Franck, R., Suquet, H., Lambert, J.-F., and Barthomeuf, D., *J. Chem. Soc. Faraday Trans.* **90**, 667 (1994).
22. Ocelli, M. L., and Finseth, D. H., *J. Catal.* **99**, 316 (1986).
23. Kloprogge, J. T., Seykens, D., Geus, J. W., and Jansen, J. B. H., *J. Non-Cryst. Solids* **142**, 87 (1992).

24. Schoonheydt, R. A., and Leeman, H., *Clay Miner.* **27**, 249 (1992).
25. Vassallo, A. M., Cole-Clarke, P. A., Pang, L. S. K., and Palmisano, A., *J. Appl. Spectrosc.* **46**, 73 (1992).
26. Frost, R. L., and Vassallo, A. M., *Clays Clay Miner.* **44**, 635 (1996).
27. Frost, R. L., Finnie, K., Collins, B., and Vassallo, A. M., *in* "The Proceedings of the 10th International Clay Conference, Adelaide, Australia" (R. W. Fitzpatrick, G. J. Churchman, and T. Eggleton, Eds.), p. 219. CSIRO Publications, 1995.
28. Čapkova, P., Driessen, R. A. J., Numan, M., Schenk, H., Weiss, Z., and Klika, Z., *Clays Clay Miner.* **46**, 232 (1998).
29. Gadsden, J. A., "Infrared Spectra of Minerals and Related Inorganic Compounds." Butterworth, London, 1975.